Supporting Information

Combined Effect of Nitrogen and Oxygen Heteroatoms and Micropores of Porous Carbon Frameworks from Schiff-Base Networks on Its High Supercapacitance

Man Zhou,[a] Xiaoyan Li,[a] Hong Zhao,[a] Jun Wang,[a] Yaping Zhao,[a,c] Fengyan Ge,[a] Zaisheng Cai*[a,b]

[a.] College of Chemistry, Chemical Engineering and Biotechnology, Donghua University, Shanghai 201620, People's Republic of China. E-mail: zshcai@dhu.edu.cn; Tel: +86-21-67792609

[b.] Key Laboratory of Textile Science & Technology (Donghua University), Ministry of Education.

[c.] Department of Materials Engineering, University of British Columbia, Vancouver, Canada

Table of Contents

Experimental Section

A. Materials

Phloroglucinol, hexamethylenetetramine, trifluoroacetic acid, 3,4,9,10-perylenetetracarboxylic dianhydride, 2,6-diamino-anthraquinone and 1-ethyl-3-methylimidazolium tetrafluoroborate were purchased from Sigma Aldrich and used without further purification. All deionized water was used in the process of synthesis and characterization.

B. Synthetic Procedures

Synthesis of triformylphloroglucinol (TFP): TFP was synthesized following previously reported procedure and characterization matched that in the literature. To dried phloroglucinol (1.002 g, 8 mmol) (2.516 g, 18 mmol) under N_2 was added 15 mL trifluoroacetic acid. The solution was heated at 100 ^{o}C for ca. 2.5 h. Approximately 25 mL of 3 M HCl was added and the solution was heated at 100 ^{o}C for 1 h. After cooling to room temperature, the solution was filtered, dichloromethane and filtered. [1]

Synthesis of polyquinoneimine (PQI): The PQI was synthesized via a DMF solution process. Specifically, 3,4,9,10-perylenetetracarboxylic dianhydride (PTDA) (0.392 g, 1 mmol) was added into DMF solution (40 mL) and heated to 140 ^{o}C. After 2,6-diamino-anthraquinone (DAAQ) (2.382 g, 10 mmol) was added to the solution, the reaction mixture was refluxed and stirred under N_2 gas at 140 ^{o}C. After 7 days, the as-obtained powder was filtrated and washed with methanol and acetone. After dried at 60 °C overnight, the brown powder of PQI was obtained.

Preparation of N, O-containing heteroatoms porous carbon framework (HPCF): HPCF@500 was synthesized at 500 °C with zinc chloride as a catalyst and solvent. Typically, PQI (0.088 g, 0.1 mmol), TFP (0.015 mg, 0.07 mmol) and zinc chloride (0.136 g, 1 mmol) were mixed in a quartz ampoule. The ampoule was evacuated by vacuum, sealed, and heated at a rate of 5 °C min^{-1} to 500 °C and maintained at this temperature for 15 h. Then, the compound was washed thoroughly with 1M HCl solution and deionized water and then dried under vacuum at 120 °C for 24 h to obtain a black powder. HPCF@400, HPCF@450, HPCF@550, and HPCF@600 were synthesized at designated temperature via similar procedures to HPCF@500.

C. Material characterization

FT-IR was carried out on a PerkinElmer Spectrum-Two (American) equipped with an ATR accessory in the range of 4000-500 cm^{-1} at a resolution of 4 cm^{-1}. The ^{1}H NMR and ^{13}C NMR were all obtained at room temperature on a Bruker Avance Spectrometer (400 MHz) using $CDCl_3$ as solvent, and calibrated at 7.26 ppm (^{1}H NMR) and 77.09 ppm (^{13}C NMR). Solid-state NMR spectra were recorded at ambient temperature on a Varian INOVA-400 spectrometer. The morphologies were observed using a field emission scanning electron microscope (FESEM, S-4800, HITACHI, Japan) and transmission electron microscope (TEM, JEM-2100, JEOL, Japan). Atomic force microscopy (AFM) measurements were conducted with a Dimension Icon AFM system (Bruker Corporation) in an in-situ way. The elemental analysis (EA) was performed with an elemental analyzer (VarioEL III). X-ray photoelectron spectroscopy (XPS) was measured by X-ray photoelectron spectroscopy (XPS, Thermo ESCALAB 250, United States). The structure was checked by X-ray diffraction (XRD, D/Max 2500PC, Rigaku, Japan) with Cu Kα (λ = 1.54056 Å). A Micromeritics ASAP 2020 surface area and porosity analyzer was utilized to study the pore structure of the samples. Brunauer-Emmett-Teller (BET) method and density functional theory (DFT) pore model were utilized to calculate the specific surface area and pore size distribution, respectively. The total pore volume was calculated from the amount adsorbed at a relative pressure Pa. 0.997.

D. Electrochemical measurements.

Preparation of HPCFs-based electrodes: Electrode films were prepared by grinding HPCFs (80 wt%, about 30 mg), acetylene black (10 wt%, Alfa Aesar), and polytetrafluoroethylene (10 wt% PTFE, 60% in water, Aldrich Co., diluted to 6% before use) in a mortar. The thin film was dried under vacuum at 120 °C for 24 h and then was pressed onto a stainless-steel wire meshes (400 mesh, 15mm×30mm) as the working electrode.

Electrochemical measurements for single electrode: Electrochemical measurements of single electrode were performed in a three-electrode system, which comprised a HPCFs film pressed onto a titanium mesh as the working electrode, a platinum sheet (10 mm×20 mm) as the counter electrode, and aqueous Hg/Hg_2SO_4 as the reference electrode. The three electrodes were immersed in a beaker containing 1 M H_2SO_4 solution. Cyclic voltammograms (CV), galvanostatic charge-discharge curves, and Nyquist plots collected on a CHI 660D electrochemical workstation at room temperature. The specific capacitance (C, F g^{-1}) was calculated from the slope of the discharge curve using: $C = It/mV$, where I (unit: A) is the discharge current, m (unit: g) is the mass of HPCFs in the working electrodes, t (unit: s) is the discharge time, and V (unit: V) is the discharge voltage.

Electrochemical evaluation for symmetric supercapacitors: Electrochemical measurements of the symmetric supercapacitors were performed in a traditional two-electrode symmetric super capacitor system (a coin-type cell of 2032 size) with room temperature ionic liquid, 1-ethyl-3-methylimidazolium tetrafluoroborate (EMIMBF$_4$) as the electrolyte. Typically, two electrode tablets with exactly the same mass were pressed onto stainless steel wire meshes respectively as the two symmetric working electrodes. The two electrodes separated by a cellulose separator (thickness of 30 μm) were soaked into EMIMBF4 electrolyte and assembled into a coin-type cell.

E. NMR Spectroscopy

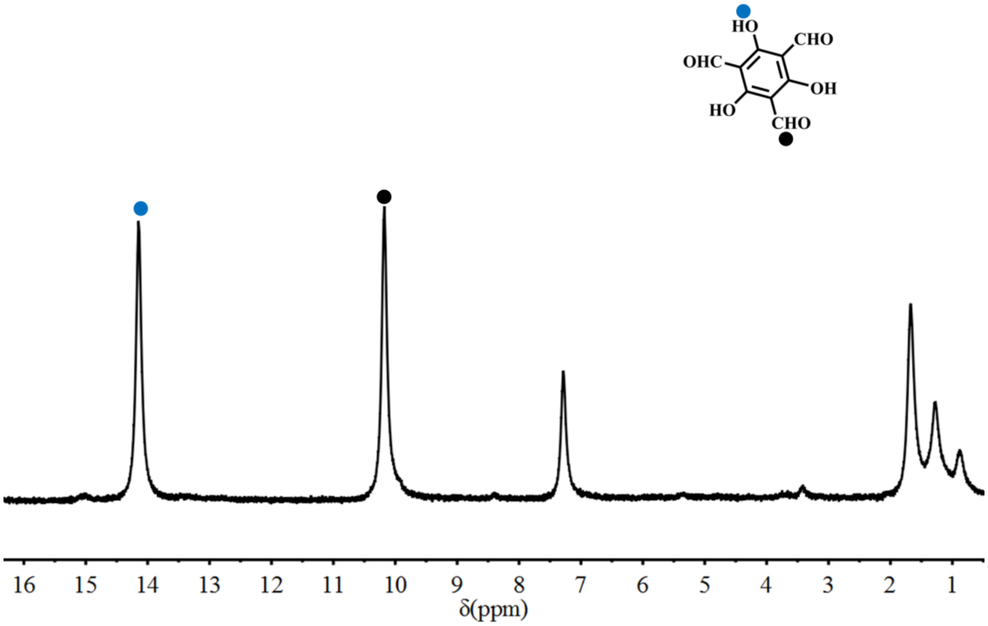

Figure S1. ^{1}H-NMR spectrum (CDCl$_3$, 400 MHz) of TFP.

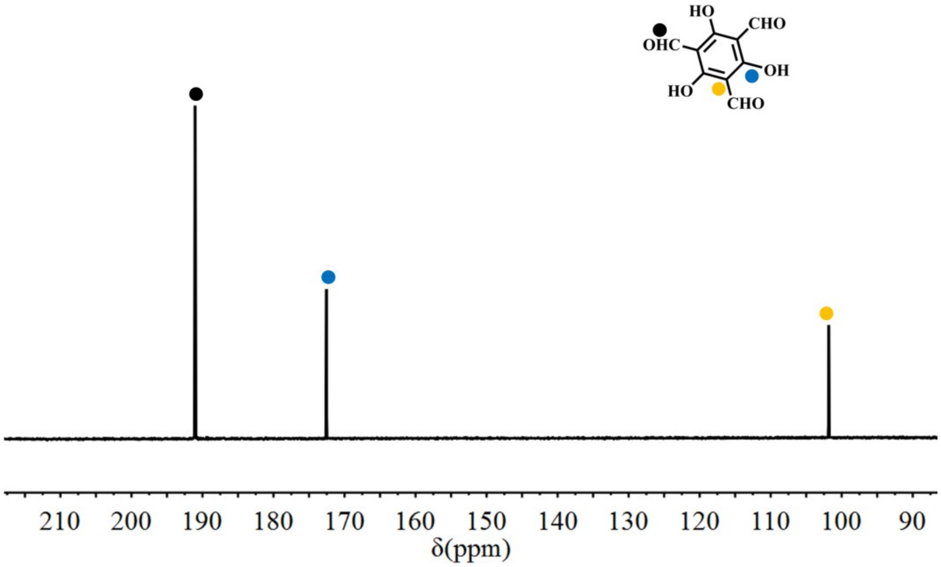

Figure S2. ^{13}C-NMR spectrum (CDCl$_3$, 400 MHz) of TFP.

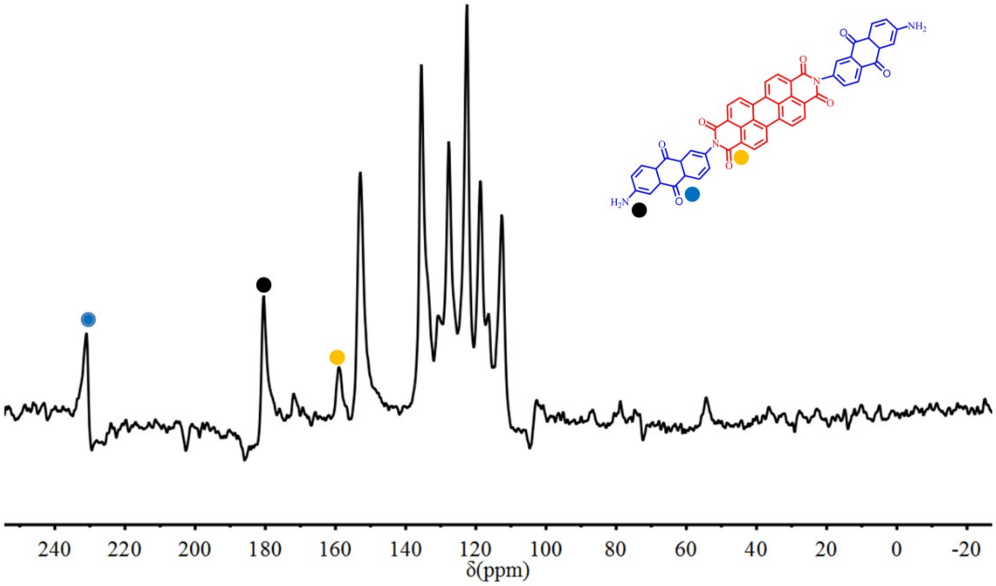

Figure S3. Solid-state ^{13}C-NMR spectrum of PQI.

F. FI-IR Spectroscopy

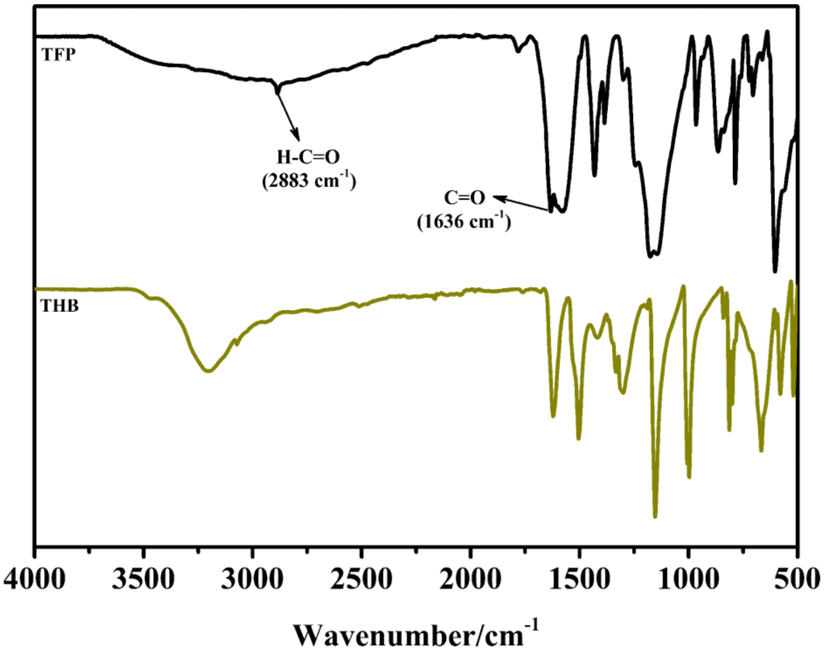

Figure S4. FT-IR of TFP (black), THB (dark yellow).

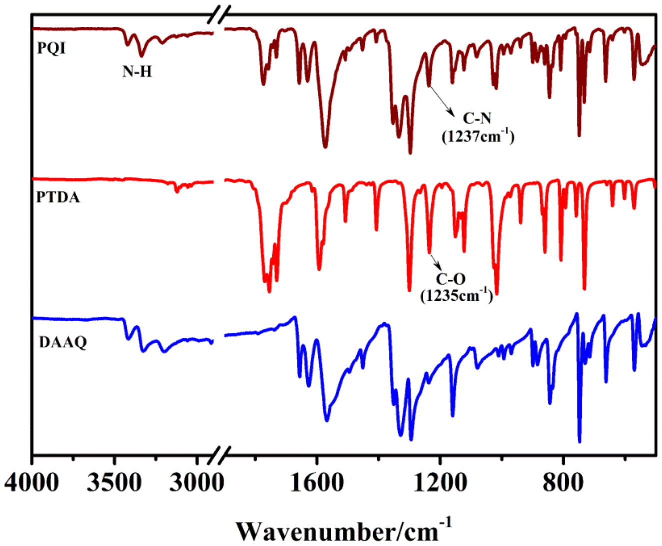

Figure S5. FT-IR of DAAQ (blue), PTDA (red) and PQI (wine).

G. XPS spectra

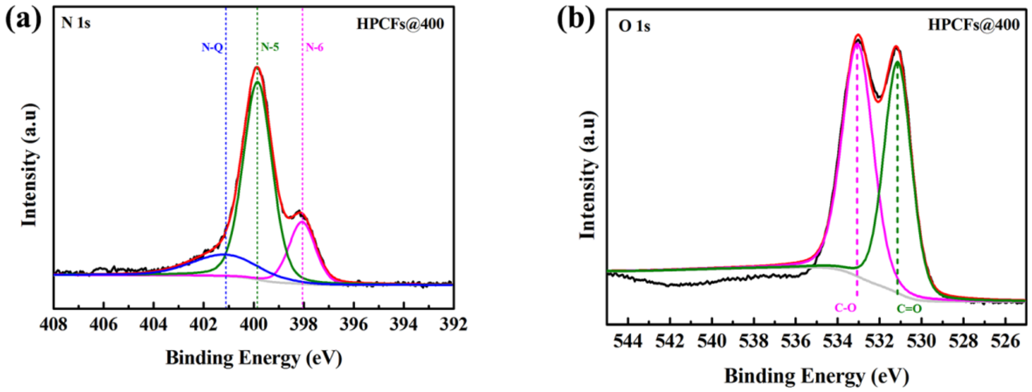

Figure S6. XPS typical N 1s (a) and O 1s (b) deconvolution of HPCF@400.

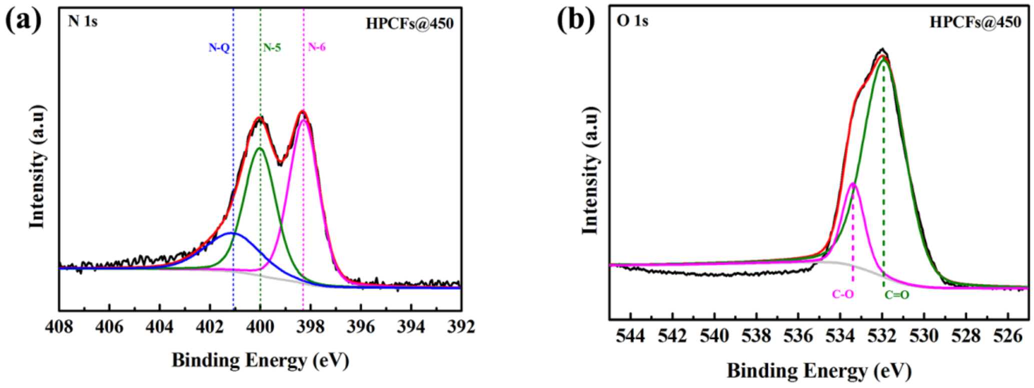

Figure S7. XPS typical N 1s (a) and O 1s (b) deconvolution of HPCF@450

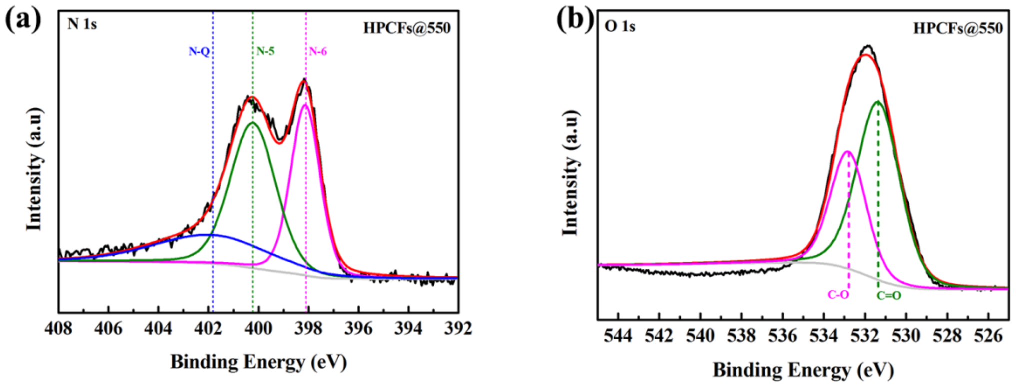

Figure S8. XPS typical N 1s (a) and O 1s (b) deconvolution of HPCF@550

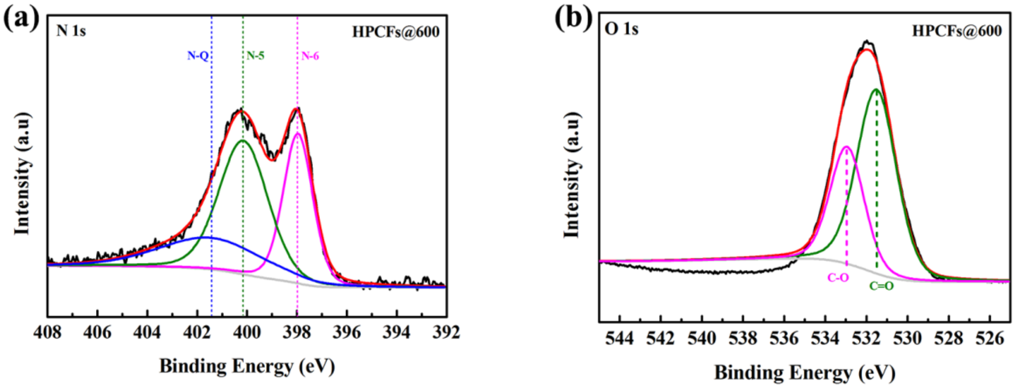

Figure S9. XPS typical N 1s (a) and O 1s (b) deconvolution of HPCF@600

H. XPS and Elemental Analyzes Date

Table S1. Relative surface concentrations of nitrogen and oxygen species obtained by fitting the N1s and O1s core level XPS spectra.

Sample	**N-6**	**N-5**	**N-Q**	**O-I**	**O-II**
PQI-TFP	22.28	77.72	-	67.30	32.70
HPCF@400	16.42	65.01	18.56	50.28	49.72
HPCF@450	44.4	36.38	19.20	61.85	38.15
HPCF@500	33.22	46.27	20.51	53.55	46.45
HPCF@550	33.60	44.12	22.28	67.65	32.35
HPCF@600	31.03	45.75	23.21	63.55	36.45

Table S2. Carbon, hydrogen, nitrogen, and oxygen contents [%] in the studied samples obtained from elemental analyzes and X-ray photoelectron spectroscopy (XPS) (hydrogen is not included).

Sample	C	H	N	O	N/C	O/C	C_{XPS}	N_{XPS}	O_{XPS}
PQI-TFP	67.51	3.05	6.47	22.97	0.0958	0.3402	81.25	3.93	14.83
HPCF@400	66.61	3.05	6.60	23.74	0.0991	0.3564	78.84	6.05	15.11
HPCF@450	65.20	3.23	6.53	25.04	0.1001	0.3840	83.27	5.06	11.67
HPCF@500	66.08	3.75	6.42	23.75	0.0971	0.3594	82.47	5.43	12.10
HPCF@550	64.52	3.07	6.53	25.88	0.1012	0.4011	83.02	5.89	11.09
HPCF@600	65.66	2.01	6.48	25.85	0.0987	0.3037	79.30	5.82	14.88

I. Transmission Electron Microscope

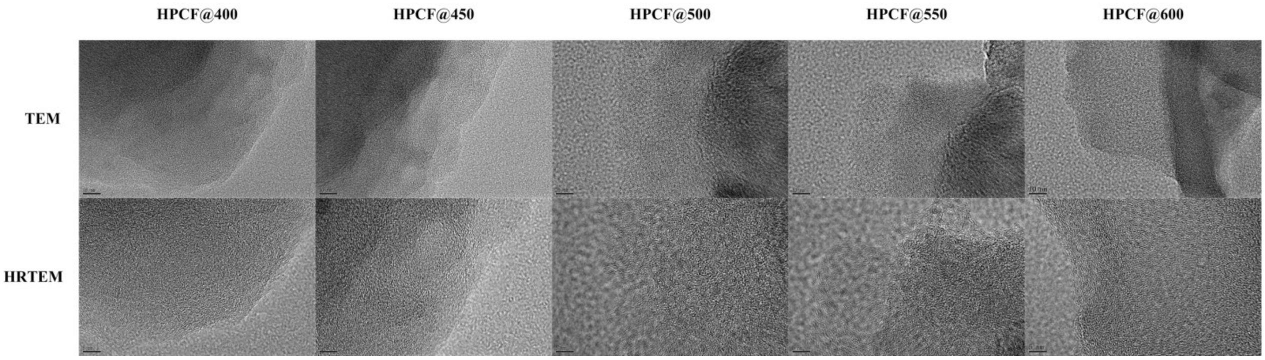

Figure S10. High-resolution transmission electron microscopy (HR-TEM) images of HPCF@400, HPCF@450, HPCF@500, HPCF@550 and HPCF@600.

J. Electrochemical Data

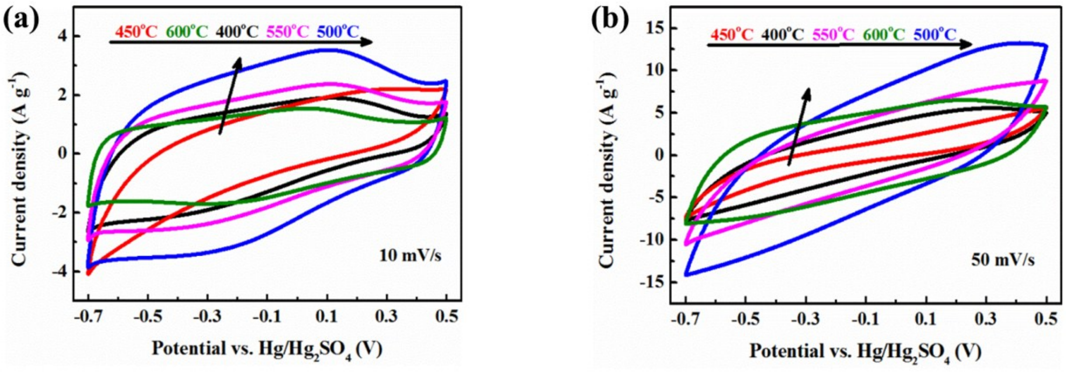

Figure S11. (a) Cyclic voltammograms of HPCFs at 10 mV s^{-1}. (b) Cyclic voltammograms of HPCFs at 50 mV s^{-1}.

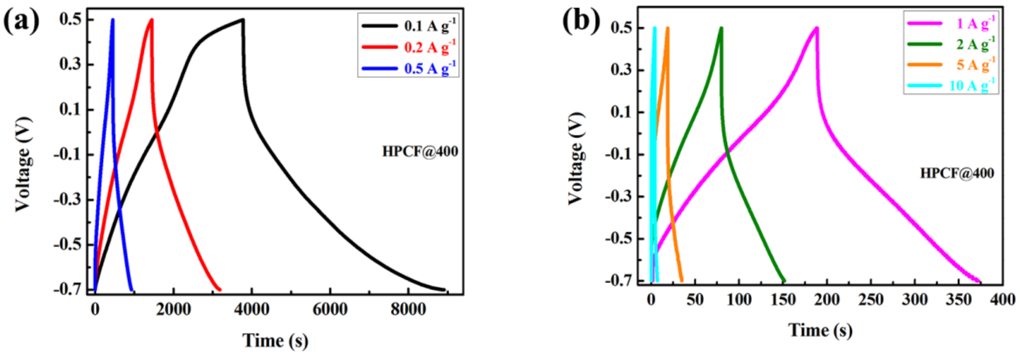

Figure S12. (a) Galvanostatic charge-discharge curves of HPCF@400 at 0.1, 0.2 and 0.5 A g^{-1} (b) Galvanostatic charge-discharge curves of HPCF@400 at 1, 2, 5 and 10 A g^{-1}.

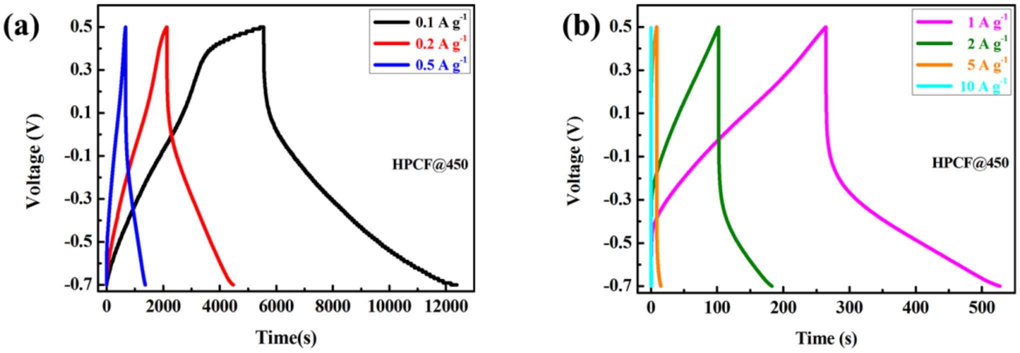

Figure S13. (a) Galvanostatic charge-discharge curves of HPCF@450 at 0.1, 0.2 and 0.5 A g^{-1} (b) Galvanostatic charge-discharge curves of HPCF@450 at 1, 2, 5 and 10 A g^{-1}.

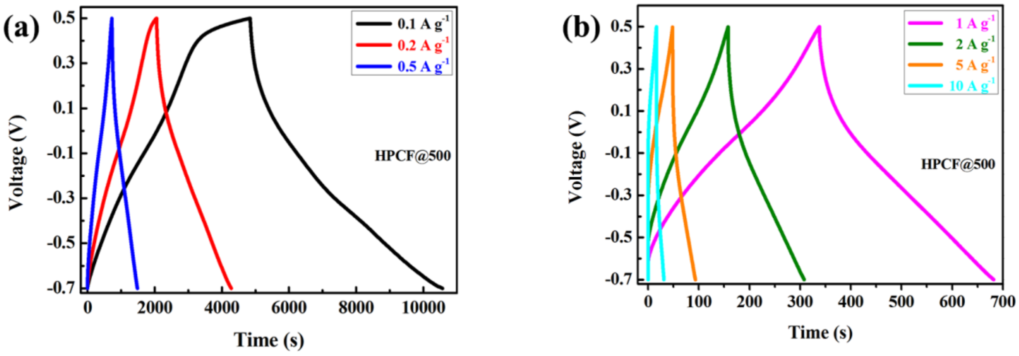

Figure S14. (a) Galvanostatic charge-discharge curves of HPCF@500 at 0.1, 0.2 and 0.5 A g^{-1} (b) Galvanostatic charge-discharge curves of HPCF@500 at 1, 2, 5 and 10 A g^{-1}.

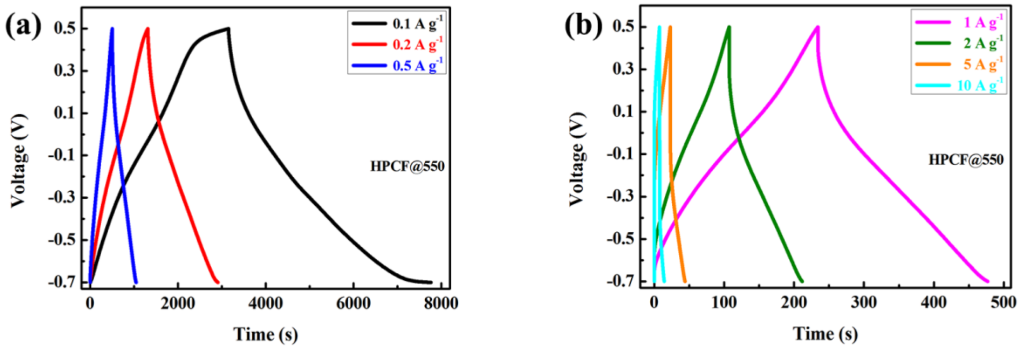

Figure S15. (a) Galvanostatic charge-discharge curves of HPCF@550 at 0.1, 0.2 and 0.5 A g^{-1} (b) Galvanostatic charge-discharge curves of HPCF@550 at 1, 2, 5 and 10 A g^{-1}.

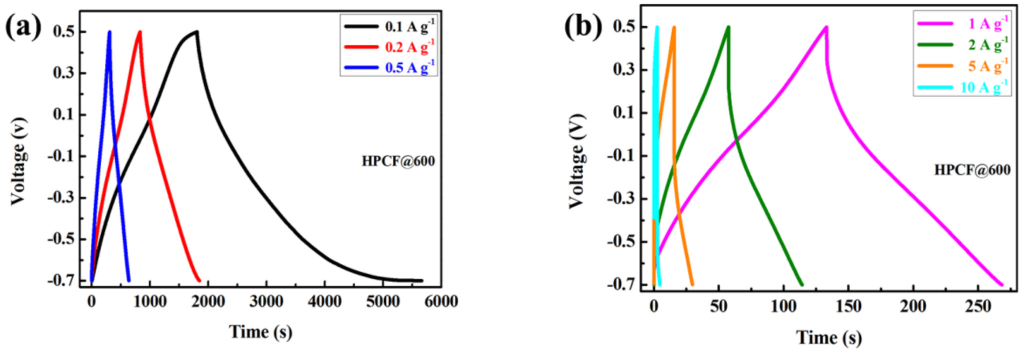

Figure S16. (a) Galvanostatic charge-discharge curves of HPCF@600 at 0.1, 0.2 and 0.5 A g^{-1}. (b) Galvanostatic charge-discharge curves of HPCF@600 at 1, 2, 5 and 10 A g^{-1}.

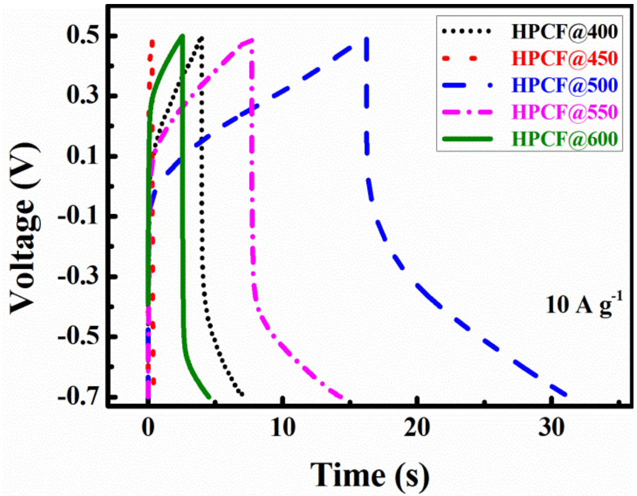

Figure S17. Galvanostatic charge-discharge curves of HPCFs at 10 A g^{-1}.

K. Reactions of oxygen-related and nitrogen-related functional groups under acidic conditions.

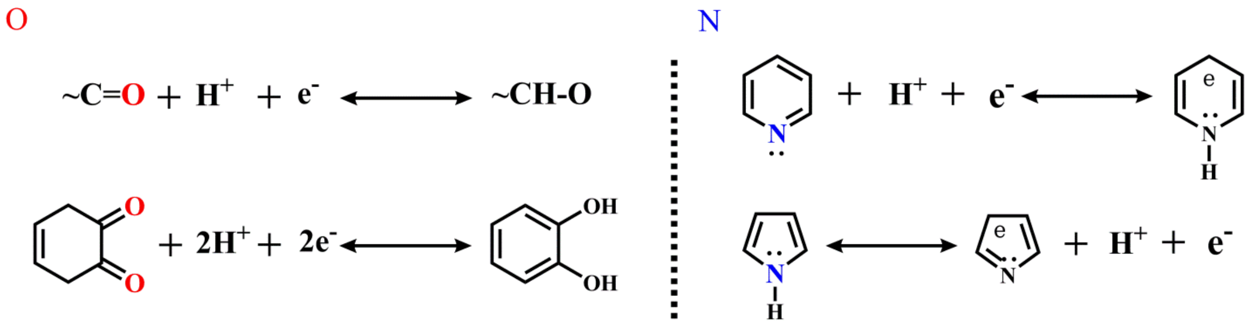

Figure S18. Reactions of oxygen-related and nitrogen-related functional groups under acidic conditions.

L. References

[1] J. H. Chong, M. Sauer, B. O. Patrick, M. J. Maclachlan, *Organic Letters* **2003**, 5, 3823.